Assessment of the Impacts of Climate Change on Gibe-III Reservoir Using Reliability, Resilience and Vulnerability (RRV) Indices

MelkamuTeshomeAyana, NegashWageshoAmencho, Abdella Kemal Mohammed

Abstract— The main objective of this study is to assess the possible impacts of future climate change on Gibe-III reservoir by using the reliability, resilience and vulnerability indices (RRV-criteria). Three greenhouse gas (GHG) emission scenarios; RCP2.6, RCP 4.5 and RCP8.5 from CORDEX archive were used to generate the future climate variables. A hydrological model, HBV was utilized to simulate the water balance. The model was calibrated and validated at Abelti gauge station using 1985-2004 observed hydro-meteorological data. The performance of the model was resulted with NSE of 0.76. Future climate projection as compared to the base line period (1986-2020) shows an increasing trend for both Tmax and Tmin. However, precipitation projection didn't manifest a systematic increase or decreasing trend during 2021-2065. The net inflow volume to Gibe-III reservoir was estimated by subtracting evaporation loss from Gibe-I and Gibe-III reservoir from the total flow generated. The result shows an average decrease by 9.8% under all scenarios. The main reason for this change is the cumulative effect of increase in Tavg contributing to high evaporation loss and decrease in annual precipitation. On average for both RCP2.6 and RCP4.5 emission scenarios, the time based reliability of Gibe-III reservoir shows that more than 75% of the time the target demand is fully supplied. The resilience of the reservoir is ~20% which indicates the reservoir may need long time to recover itself from failure to meet the demand. The dimensionless vulnerability of the reservoir falls under 50% implying that the reservoir may not face a challenge from shortage of flow to meet the demand in its simulation period.

Index Terms— Climate Change, Gibe-III, GHG, HBV, RCP and RRV.

1. Introduction

Climate change refers to a change in the state of the climate that can be identified by changes in the mean or the variability of its properties. This change may persist for an extended period, typically decade. Influences such as changes in solar radiation and volcanism, occur naturally and contribute to the natural variability of the climate system. Changes in temperature and precipitation patterns as consequence of increased greenhouse gases (GHG) concentration may affect the hydrological processes and availability of water resources for various purposes (IPCC, 2014).

According to the IPCC fifth assessment report, AR5 there are many indicators of climate change. These include physical responses such as changes in the surface temperature, atmospheric water vapour, precipitation, severe events, glaciers, ocean and land ice, and sea level rise. It has been speculated that the mean global surface air temperature for the period 2016-2035 may be higher than the observed mean for 1850-1900 by 1^{o}C to 1.5^{o}C.

Water scarcity and fragility, unequal distribution in space and time and its mismanagement are regarded as serious issues in most developing countries. These issues are mainly due to population pressure and fast urbanization as well as industrial and agricultural development (Raje and Mujumdar, 2009). The competing demand for water has increased manifold in developing countries, with high economic growth, change in lifestyles, industrialization, and urbanization. Available supplies are under great stress as a result of population growth, unsustainable consumption patterns and poor management practices.

Like many other developing country, Ethiopia has been utilizing large volume of water for different development activities in the past ten years. For instance, the cascade reservoirs on Omo Gibe River are examples of those developments in the country. In the upper reach of the river basin, cascade of hydropower schemes, i.e., Gibe-I, Gibe-II, and Gibe-III are operating while Gibe- IV and Gibe-V are under serious national commitment to be realized soon. The lower reach is being developed for large scale irrigation farming covering 175,000 hectares of land that will supply sugarcane as raw material to ten sugar factories out of which six are currently under construction. Such very aspiring yet demanding plans of the government in the basin, may lead to water stress unless managed sustainably. In addition to this, the impact of changing global weather pattern may exacerbate the water stresses.

The potential impact of climate change on the ability to meet future demands for high quality drinking water and satisfy other competing goals for surface water supplies is an issue of importance in many regions.

Modern agriculture largely depends on available water resources while large part of the country is categorized as arid and semi-arid region highly prone to drought and desertification. Search for alternative sources of livelihoods as a result of increasing population pressure ultimately degrades the fragile ecosystem to greater extent. Climate variability in terms of flood and drought has been imposing a significant challenge to Ethiopia by limiting the development efforts and adaptive mechanisms towards poverty reduction, food security and water & energy supply. Above all the level of awareness about the environmental degradation and climate change and subsequent responses the people are undertaking are still very low. Climate change and its impacts, the level of vulnerability, adaptive strategies and mitigation measures are not yet sufficiently addressed.

Recently, flood events in Dire Dawa region, lower Awash and Omo basin highly affected the community and threatened their livelihoods by large. The problem depends on the river system topography of the plain and flow phenomena and land cover. Flood in Omo-Rate and Nyangatom killed a lot of people and domestic animal in 2006. Main problem of flooding in Omo-Rate is inundation caused by spilling of the river Omo-Gibe as well as its tributaries

Flood caused due to the overflow of Omo river killed more than 364 people in Omo zone of the southern nations nationalist and people state in 2006. The flood bursts-out from the Omo River flooded ten Kebeles in DasenechWoreda and killed 364 people the people confirmed dead in the deluded reached the stated number on 2:00 pm Tuesday 15 August 2006. An additional 3,000 cattle were reported to have been lost by the floods. Over 3,730 heads of cattle and pack animals including Bees were killed by the flood that also swept crops on 4,240 hectares of land due to this flood which was occurred in that year.

Considering the use of water resource in a sustainable manner and projecting the future likelihood patterns of this resource under different scenarios can help to mitigate and adapt the multidimensional impact of climate change. Omo-Gibe River basin is one of the highest socioeconomic development sites due to its tremendous potential for hydropower and irrigation. However, in recent years, the climate variations induced hydrological variability poses a challenge on decision making for planning, design and operation of hydropower plants irrigation projects and sustainable utilization of the basins potential. Therefore, there should be a better understanding and projection of all the systems which can lead to a sustainable and optimal use of water and other resources for the intended purpose.

The main objective of this study is to assess the effect of climate change on the future availability of water resources and the magnitude and frequency of extreme events for various plausible scenarios. Specifically,

1. To carry out catchment level hydrologic modeling using HBV model and hence, estimate inflow volume in to Gibe-III reservoir
2 To assess possible impacts of climate change on the surface water resources availability, flow magnitude and timing of the major flow events at upper reaches of Omo-Gibe basin for the next 45 years (2020 to 2065).

2. METHODS AND MATERIALS

2.1 Description of the study area

The Upper Omo-Gibe basin is one of the major river basins in Ethiopia and is situated in the south western part of the country covering parts of SNNPR and Oromia region. The basin covers an area of 33,736 km^2. The basin lies in between 747065.63N &1035665.63N latitude and between 434855.11E &129855.11E longitude in UTM. Rainfall in Omo-Gibe basin varies from over 1900 mm per annum in the north central areas to less than 450mm per annum in the south. The amount of rainfall decreases throughout Gibe-III catchments with a decrease in elevation. Moreover, the rainfall regime is unimodal for the northern and central parts of the basin and bimodal for south. The mean annual temperature in basin varies from 16^{0}C in the highlands of the north to over 30^{0}C in the lowlands of the south. The total mean annual flow from Gibe-III river basin is estimated to be 13.8 BMC (Kemal, 2013).

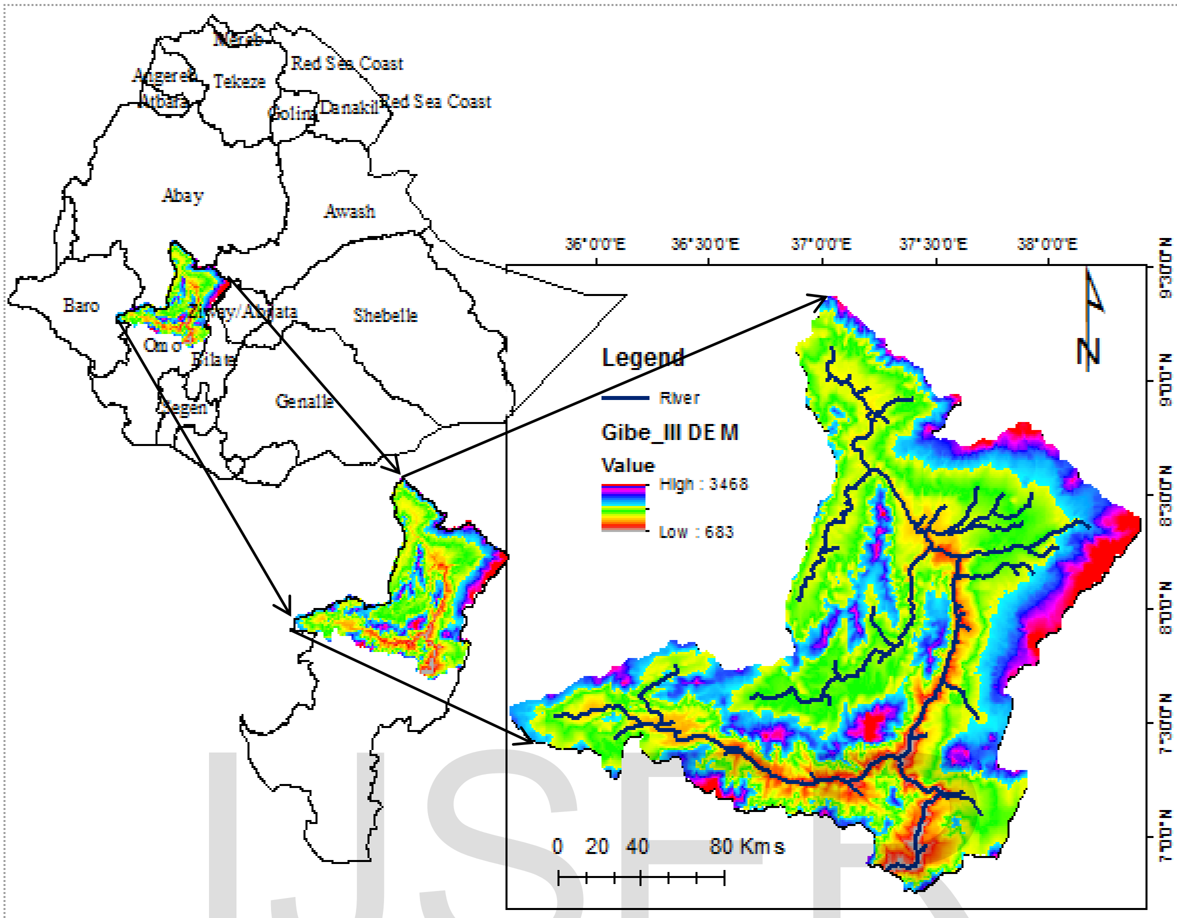

Fig2.1 Gibe-III watershed with its drainage system

2.2Methods and Data used

More than 20 meteorological stations nearby the watershed were identified and used for this study. Three major hydrological stations namelyGreat Gibe at Abelti, Gojjeb and Wabe in the upper part of the basin were used. Using Gibe-III meteorological stations and Gibe at Abelti; HBV hydrological model parameters were optimized.Thereafter, by using the optimized parameters, inflow for the unguaged part of the basin was estimated. Finally, the future inflow volume in to Gibe-III reservoirwas generated and used to estimate the reservoir performance under climate change.

a. Model performance evaluation

For evaluation of the performance of the model, three efficiency measuring techniques; Nash Sutcliffe Efficiency (NSE), Coefficient of determination (R2), percent in volume difference (D) were used.

Nash-Sutcliffe efficiency (NSE): The efficiency, NSE proposed by Nash and Sutcliffe (1970) is defined as one minus the sum of the absolute squared differences between the predicted and observed values normalized by the variance of the observed values during the period under investigation. Moriasi et al (2007) recommended for monthly time steps that NSE values between 0.75 and 1 is very good and NSE-value between 0.65 and 0.75 is good.

$$\mathrm{NSE} = 1 - \frac{\sum_{i=1}^{n}(O_i - P_i)^2}{\sum_{i=1}^{n}(O_i - \overline{O})^2} \qquad (2.1)$$

Where, Oi is observed flow at i^{th} period, Pi is simulated flow at the i^{th} period and $\overline{O}$is mean of the observed flow

Coefficient of determination (R^2): The coefficient of determination R^2 is defined as the squared value of the coefficient of correlation. It can also be expressed as the squared ratio between the covariance and the multiplied standard deviations of the observed and predicted values. It is calculated as:

$$R^2 = \frac{[\sum_{i=1}^{n}(Q_s - \bar{Q}_s)(Q_o - \bar{Q}_o)]^2}{[\sum_{i=1}^{n}(Q_s - \bar{Q}_s)]^2[\sum_{i=1}^{n}(Q_o - \bar{Q}_o)]^2} \quad (2.2)$$

Moriasi et al (2007) recommended for monthly time steps that R^2 values between 0.75 and 1 is very good and R^2-value between 0.65 and 0.75 is good.

The percent difference for a quantity(D): The percent difference over a specified period with total days calculated from measured and simulated values of the quantity in each model time step as: A percent difference between +5% and -5% indicates that a model performs well while in between +5% and +10% and -5% and -10% indicates a model with reasonable performance.

$$D = \left[\frac{\sum_{i=1}^{n} Q_o - \sum_{i=1}^{n} Q_s}{\sum_{i=1}^{n} Q_o}\right] * 100\% \quad (2.3)$$

b. Flow Transfer to the dam site

Omo Gibe basin is one of the most poorly gauged basins in Ethiopia. The data from some of the station doesn't have good quality and/or there is no sufficient hydrological station in the basin. Some are not located at rivers confluence and dam sites (Kemal, 2013). Hence, transferring stream flow data to the point of interest in many reservoirs become important. To transfer flow data to Gibe-III near dam site, two major tasks were done. Firstly, flow from Gojeb near Shebe was transposed to Gojeb near Gojeb dam site by using area ratio method (Eqn 2.4). Secondly, flow from each basin was transferred to Gibe-III near dam site by using Muskingum routing technique (Eqn2.5). Finally, the entire flow transferred to Gibe-III dam site were summed-up to obtain the total approximate flow at Gibe-III near dam site.

$$\text{Qsite} = \text{Qgauged} * \left(\frac{A_{\text{unguaged}}}{A_{\text{gauged}}}\right)^n \quad (2.4)$$

Where,A_{site} is drainage area at site of interest, Aguage is drainage area of the guage site, Q_{site} is discharge at site of interest and Q_{guage} is discharge at guage site. n is a value which varies between 0.6 and 1.2. n value of 0.95 was used for this particular project.

The general Muskingum Eqn was stated below where the corresponding coefficients values were adopted from Kemal (2013).

$$\text{Q out}(t+1) = C1 * \text{Qin}(t+1) + C2 * \text{Qin}(t) + C3 * \text{Qout}(t) \quad (2.5)$$

2.2.1Impact Assessment and Performance Indices

The analysis of potential climate change impact on the Hydropower requires simulation of the water balance under different climate scenarios. There are different measures for assessing system performance. Hence, the study used three performance indices that will be used to evaluate the climate change impact on reservoir comparatively, these are; Reliability, Resilience and Vulnerability indices.

Reliability, Re, is defined as the probability that a water supply system will be able to meet, within the simulation period, the target demand in any given interval of time (often a year or a month). There are several measures of reliability, which are defined as follows.

Time-based reliability, Rt, considers the proportion of intervals during the simulation period that the reservoir can meet the target demand. A general expression for estimating this metric is:

$$R_t = \frac{N_s}{N} ; 0 \leq R_t \leq 1 \quad (2.6)$$

Where, Rt is the time-based reliability, Ns is the number of intervals that the target demand was fully met and N is the total number of intervals covering the historical or simulation analysis period. When the time interval is monthly or annual, we speak about a monthly or an annual time-based reliability, respectively.

Volumetric reliability, Rv, is defined as the volume of water supplied to a demand center divided by the total target demand during the entire simulation period, i.e.

$$R_v = 1 - \frac{\sum_{i=1}^{n}[D_i - D_i']}{D_i} ; 0 \leq R_v \leq 1 \quad (2.7)$$

Where, Rv is the volumetric reliability, D_i is the target demand during ith period, i D_i' is the volume actually supplied during the ith period and n is the number of time intervals in the simulation, so that Rv=1 if D_i is totally satisfied, i.e. $D_i = D_i'$for all i. It should be noted that R_v will always be equal to or greater than Rt because during a time interval in which a failure is recorded some release, although lower than the target demand, may be still made.

Resilience, φ, is a metric defining how quickly a reservoir will recover from a failure. The measure adopted in this study is used

$$\varphi = \frac{f_s}{f_d}; fd \neq 0 \quad (2.8)$$

where φ is resilience, fs is the number of individual continuous sequences of failure periods and fd is the total duration of all the failures, in other words, φ is the inverse of the average failure duration. Resilience is the probability of a year of success following a year of failure.

Vulnerability, η′ the metric known as vulnerability measures the average volumetric severity of failure during a failure period.

$$\eta' = \frac{\sum_{j=1}^{f_s} \max(Sj)}{f_s} \quad (2.9)$$

Where η′ is the vulnerability, is the volumetric shortfall during jth continuous failure sequence and fs is the number of continuous failure sequences. Averages out the maximum short fall over all the continuous failure periods, then a reduction in fs will cause η′ to increase when the numerator in Eq. (2.9) remains unchanged. A practical situation where, this may occur is when the reservoir capacity is increased, with all other factors remaining constant. One way to avoid this anomaly is to remove the averaging in Eq. (2.9). Another point to note about Eq. (2.9) is that η′ is in volumetric units; a more useful expression of vulnerability is its dimensionless form given by:

$$\eta = \frac{\eta'}{Df}; 0 \leq \eta \leq 1 \quad (2.10)$$

Where, η is the dimensionless vulnerability metric, known as the vulnerability ratio in this paper, and Dfis the (constant) target demand during failure. (Note that Df=D, i.e. target demand is the drought and non-drought period.

2.2.2Data Used for this Study

The data used for this study includes: GIS data, Hydro-meteorological data, reservoir physical data, plant data and others. GIS data such as Digital Elevation Model (DEM) of 30m*30m for Omo-Gibe sub-basin was downloaded from http://eijournal.com/industry-insights-trends/srtm-data-released-as-part-of-climate-summit-initiatives whereas, Ethio-river basin shape files, land use/land cover and soil data, documents of water resource development projects in the basin are all collected from Ministry of Water, Electricity and Energy (MOWIE). Design documents having geographical information concerning hydro-power and irrigation projects implemented and proposed in the basin were taken MOWIE.

Observed hydro-meteorological data series is very important in model calibrations to generate flow at different spatial and temporal points of interest. To assess the impact of climate change on Omo- Gibe sub-basins hydrological data of three stations located at the upper part of the basin were selected. These includes: Gibe at Abelti, Gojeb at Shebe, and Wabi at Wolkite. More than twenty meteorological stations data located inside and nearby the basin were collected for this particular work. Table 2.1 shows the meteorological data used and record length. The data length covers duration of 28 to 32years. In general, hydrological data for the selected stations in the upper Omo-Gibe basin reveals good quality for the periods 1985-2004. Hence, the same period hydro-meteorological data were used for model analysis in this work.

Table 2.1: Meteorological stations used, location and their record length

S. No	Stations	Location		Data Availability		Total years
		Long.	Lat.	From	To	
1	Assendabo	303329	857073	1984	2014	31
2	Bonga	224251	857472	1985	2014	30
3	Cheka	323581	864366	1987	2014	28
4	Chekorsa	249920	842576	1984	2014	31
5	Dedo	264587	831442	1984	2014	31
6	Durame	384070	795991	1984	2006	23
7	Gedo	330447	997532	1984	2015	32
8	Gibe farm	340286	910346	1984	2014	31
9	Hossana	373551	836629	1984	2015	32
10	Jimma	259150	847986	1984	2015	32
11	Jinka	228665	637995	1984	2015	32
12	Kumbi	332889	897508	1984	2015	32
13	LimmuSeka	290740	917965	1985	2014	30
14	Meteso	264338	777934	1984	2015	32
15	Morka	312703	710053	1984	2014	31
16	Sawula	261172	697414	1987	2015	29
17	Shebe	225935	829798	1984	2014	31
18	Woliso	388110	945250	1984	2014	31
19	Wolkite	329225	898996	1984	2015	32
20	Yaya Tore	338501	925135	1984	2014	31

Bias correction of precipitation and temperature data for RCP application to the Omo-Gibe basin

Precipitation bias correction: Nowadays, modelers are aware of the uncertainty involved in modeling, and the necessity to quantify the model output reliability. Spatially distributed models are often forced with regional climate model output (e.g., REMO Jacob, 2001), because observations are scarce on the spatial and temporal resolution at which these spatially distributed models are run. The bias correction applied in this study is based on the method proposed by Leander and Buishand (2007) for a Meuse basin study. Bias in precipitation and temperature was found to vary spatially. Hence, bias correction for Omo-Gibe basin precipitation was made by using power transformation method. Generally, from fifteen years (1986-2000) 450 (30days*15years) sample data were considered. Accordingly the result reveals a good coherence in terms of mean deviation throughout the year whereas slightly significant coefficient of variation is observed during January, February, October and November months (Fig 2.1).

Temperature bias correction: For correcting the daily temperature a different technique is used to correct the data from CORDEX archive. The correction of temperature only involves shifting and scaling to adjust the mean and variance (Leander and Buishand, 2007). The correlation coefficients were obtained for each month and applied to correct each months corresponding temperature. Then the mean monthly temperature was calculated from the minimum and maximum temperature for the basin (Fig 2.2).

ISSN 2229-5518

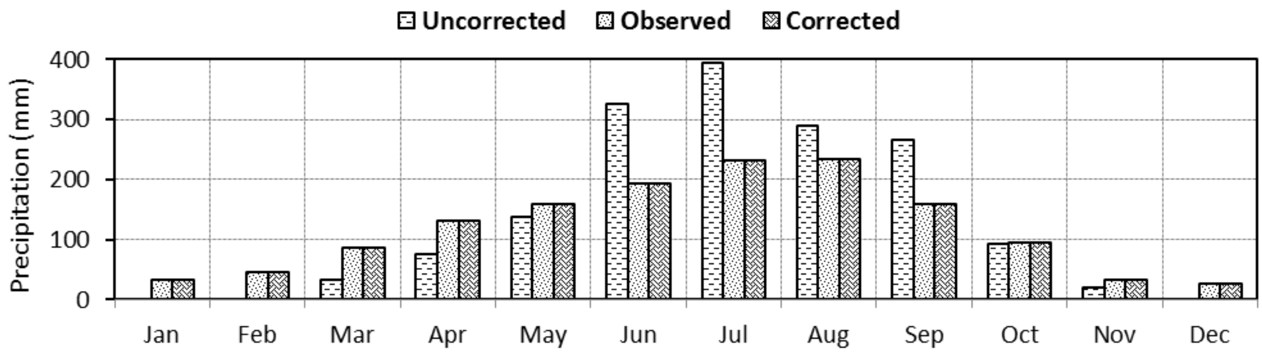

Fig 2.1: Comparison of observed and corrected rainfall for Gibe-III basin (1986-2000)

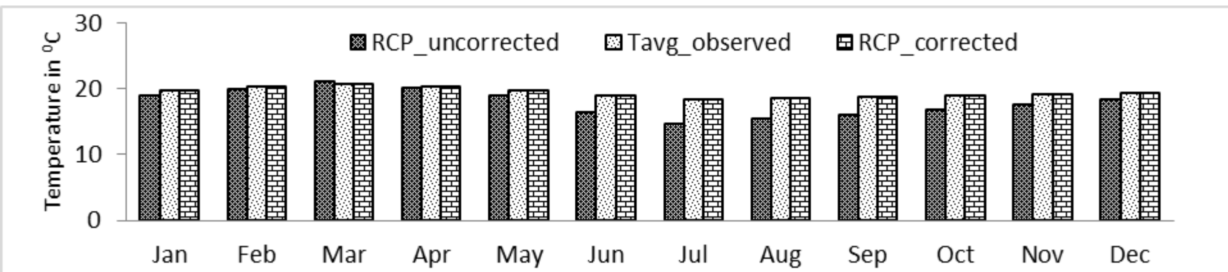

Fig 2.2: Comparison of observed and corrected mean monthly temperature

Areal Rainfall Estimation

Different methods are available to determine the areal rainfall over the catchments from the rain gauge measurement: Arithmetic Mean, Thiesson Polygon, Isohyetal, Grid Point, Percent Normal, Hypsometric, etc. are available for estimating average precipitation over a drainage basin (Shaw, 1988). Choice of methods requires judgment in consideration of quality and nature of the data, and the importance, use, and required precision of the result. For this study, the Theisson polygon method was used to estimate the areal rainfall. If there are n-number of stations and n-polygons, the average depth of precipitation over the total area (A) is given by:P =

$$\frac{1}{A} * \sum_{i=1}^{n} A_s P_s \qquad (2.11)$$

Where, P = Areal average rainfall, Ps = Rainfall measured at sub-region, As= Area of sub-region and A = total area of sub regions.

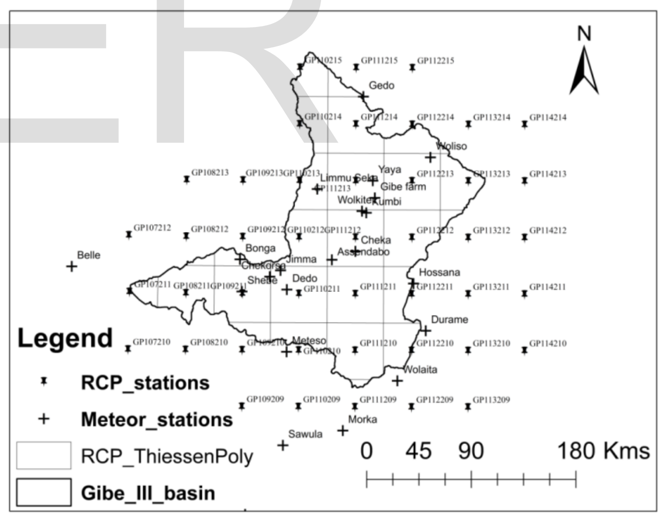

Fig2.3: Meteorological stations and RCP grid points used for Gibe-III basin

2.2.3 Reservoir inflow volume

The monthly flow at Gibe-III dam site was estimated by using the HBV model. First, the areal rainfall coverage of dam site was delineated using Arc-GIS software from 30m x 30m DEM of Omo-Gibe basin. Then, the points of each flow gauging stations were set and the areas upstream of the stations (Great Gibe near Abelti, Gojeb near Shebe, and Gibe at Wabe) were estimated from historical data. Since the ungagged portion of the basin as compared to the gauged area is very large, transposing flow to Gibe-III by area ratio method is impossible. Therefore, firstly through calibrating and validating the observed and generated inflow volume, the HBV model parameters were estimated. Secondly, assuming that the two areas have similar catchment characteristics and climatic conditions, flow for the ungagged part of the basin was estimated using HBV-model. Using Muskingum routing technique, flow from the three watersheds in addition to the simulated flow from the ungagged portion were routed to Gibe-III dam site. Finally, using different performance evaluation techniques, the routed and simulated flow at Gibe-III dam site was evaluated. Fig 2.4 shows sub-basins above Gibe-III dam site. Abelti basin covers an area of about 15866.6km2 (47%), Gojeb basin covers about 5164.4Km2 (15.3%), Wabe basin covers about 1844.2Km2 (5.5%) whereas the remaining 10861.8km2 (32.2%) is ungagged.

Net inflow in to Gibe-III reservoir: Omo-Gibe basin might be classified as one of the most poorly gauge basin in Ethiopia. If we consider only the basins upstream of Gibe-III dam site, the Un-gauged watershed portion accounts about 32.2% of the total area (33,737.6Km2). Therefore, estimating flow for the ungagged portion is important as it will be added to the routed flow from the upper three gagged basins (Abelti, Wabe and Gojeb) at Gibe-III dam site. To do this firstly, the hydrology of Abelti basin was modeled using the observed hydro-meteorological data. Then, the performance of the model was evaluated using model performance evaluation Eqns like coefficient of determination and percent difference in volume. Finally, without changing the optimized parameters obtained for Abelti basin and assuming that the two areas have similar catchment characteristics and climatic conditions, flow for the ungagged part of the basin was generated.

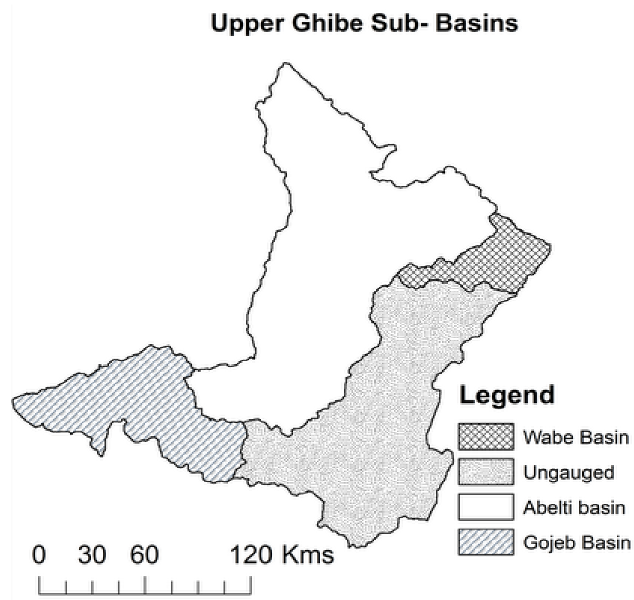

Fig2.4: Omo-Gibe Catchments upstream of the Gibe-III dam site

To estimate the net inflow in to Gibe-III reservoir, two main assumptions were adopted from literatures and different design documents (EEPCo, 2004, EEPCo, 2009 and Senayet.al, 2012). Firstly, Continuous environmental outflow of $25m^3/s$ ($64.8Mm^3$) will be released from Gibe III dam. In addition, to maintain the natural flooding conditions in the lower Omo basin, an artificial flood at the rate of $1000m^3/s$ will be released from the Gibe III reservoir for 10 days in September (864Mm3).

In general, the net inflow to Gibe-III reservoir was estimated by subtracting the sum of evaporation loss from Gibe-I and Gibe-III from the total simulated flow at Gibe-III (Eqn 2.12).

$$I_3 = I_{Sim} - E_1 - E_3 \quad (2.12)$$

Where, I_3 is net inflow at Gibe-III reservoir,I_{Sim} is simulated inflow (Mm3/m) using HBV model, E_1 and E_3 are net open water evaporation loss (Mm3/m)from Gibe-I and Gibe-III reservoirs.

In Eqn 2.12, on a monthly basis the net outflow from Gibe-III reservoir was fixed at 64.8Mm3 per each month except for September where 864Mm3 was released to maintain the natural flooding conditions in the lower Omo basin.

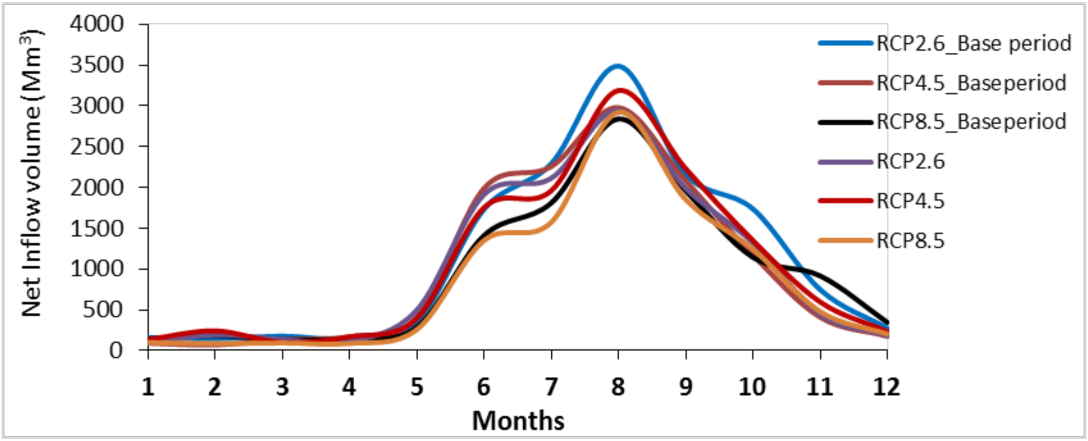

Fig 2.5: Future mean monthly net inflow volume to Gibe-III reservoir

3. RESULTS AND DISCUSSION

Future climate change of short-term (2021-2035), mid-term (2036-2050) and long-term (2051-2065) was analyzed by comparing the future downscaled climate parameter with the base period (2006-2020). The climate change estimation was made using statistically downscaled regional climate data for three Representative Concentration Pathways (Rcp2.6, Rcp4.5 and Rcp8.5) from CORDEX archive. The period from 1986-2000 was used for bias correction of RCP data. Then each future climate variables are multiplied by their corresponding coefficients to obtain bias free future climate data. The period from 2006-2020 was used as base period for comparison against the future climate data. Future scenario was developed for three periods; short-term forecast (2021-2035) mid-term forecast (2036-2050), and long-term (2051-2065) period. The Assessment was made for three climate variables; precipitation, temperature and evaporation. The hydrological variable inflow; generated from the climatic variables was also assessed for the same period as climate variables.

3.1 Precipitation Scenario

Three precipitation scenarios, the stringent mitigation scenario (RCP2.6), one intermediate scenario (RCP4.5) and one scenario with very high GHG emissions (RCP8.5) were considered to predict future climate projections. The future precipitation projection did not manifest systematic increase or decrease all over the time horizons. However, future projection has shown considerable change at monthly levels as compared to the base line period. The trend in future projections from the entire climate scenario used for this study is shown below (Fig 3.1).

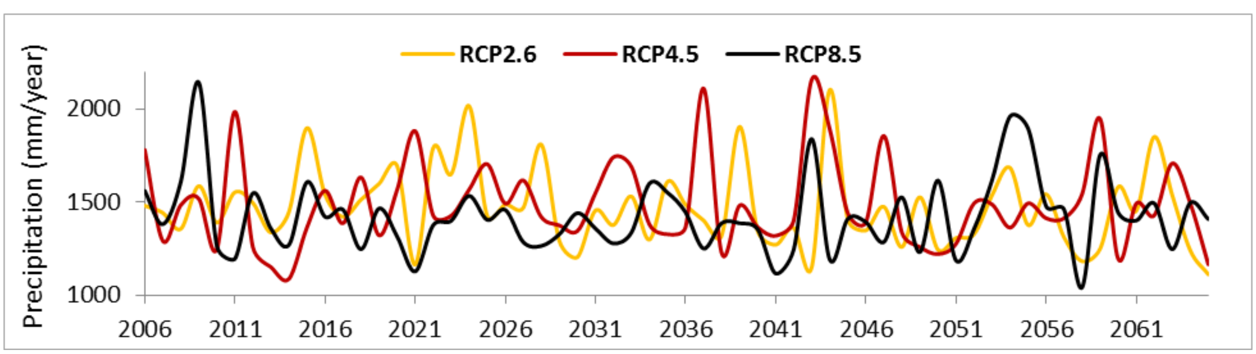

Fig 3.1: Trend in precipitation observed during 2006-2065 under different scenarios

Precipitation scenario under RCP2.6 projection reveals very high fluctuation during OND and JFM months. For instance, the mean monthly precipitation of November has shown decrement by 21.69%, 68.26% and 18.97% in a short-term, mid-term and long-term respectively. Unlike this, the climate projection under RCP 2.6 has shown some significant increment in a mid-term and long-term (27.22% in June and 44.49% in January respectively). In general, on annual basis, a decrease in precipitation magnitude by 0.56%, 5.33% and 5.64% will be expected during short-term, mid-term and long-term projections respectively.

Similar to RCP2.6 projections, the highest fluctuation is expected to occur during OND and JFM, however, RCP 4.5 projections has shown absolute increment on annual basis. Annual precipitation increases by 5.31%, 3.07% and 0.31% in a short-term, mid-term and long-term respectively.

As compared to the base period climate projection from under RCP8.5 revealed decreasing trend but certain amount of increment is expected when compared to the mid-term forecast. In general, the annual precipitation may decrease by 6.2% and 4.38% in a short-term and mid-term forecast respectively whereas shows an increase by 0.89% during long-term forecast window.

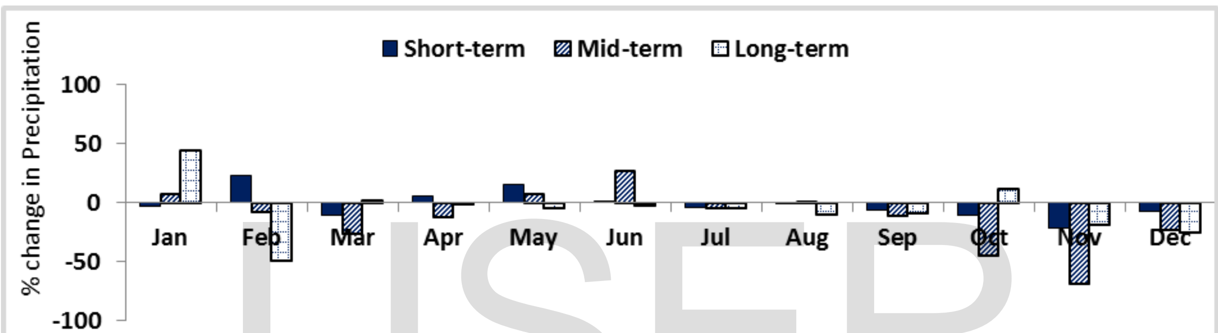

Fig3.2: Mean monthly precipitation fluxes under RCP2.6 scenario as compared to the base period

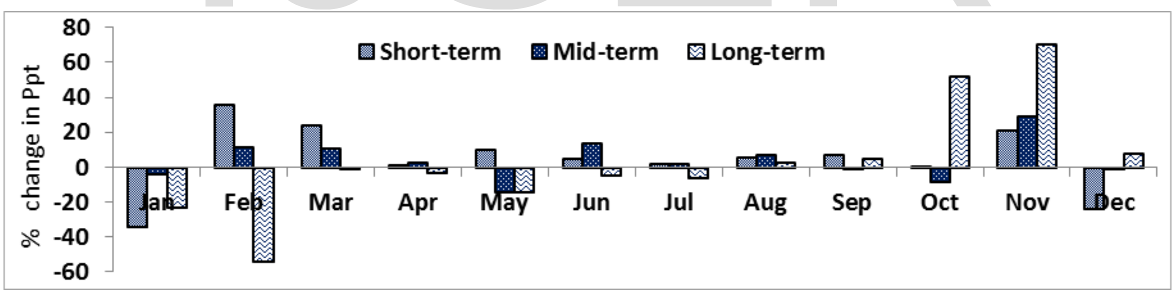

Fig3.3: Mean monthly precipitation fluxes under RCP 4.5 scenario as compared to the base period

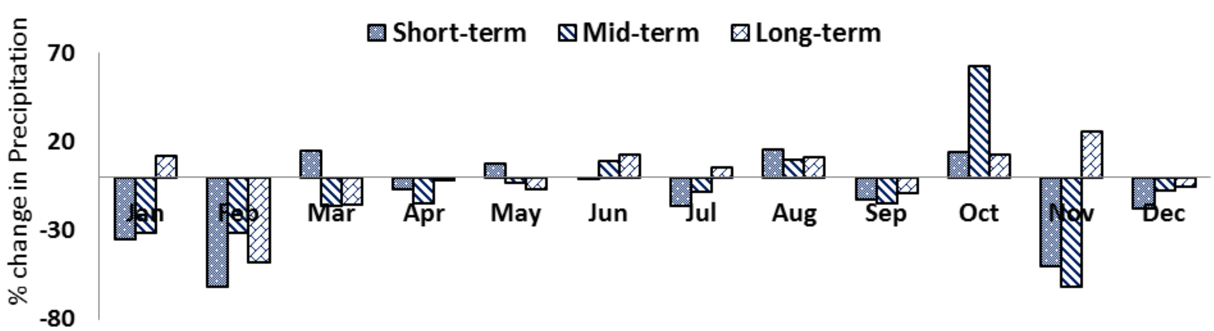

Fig3.4: Mean monthly precipitation fluxes under RCP 8.5 scenario as compared to the base period

3.2 Temperature scenario:

Maximum Temperature scenario: The projected maximum temperature has generally shown an increasing trend for the entire future time horizon. RCP8.5 which is the highest emission scenario prevail higher change in maximum temperature trend at the end of 2065 than the RCP2.6 (stringent emission) scenario.

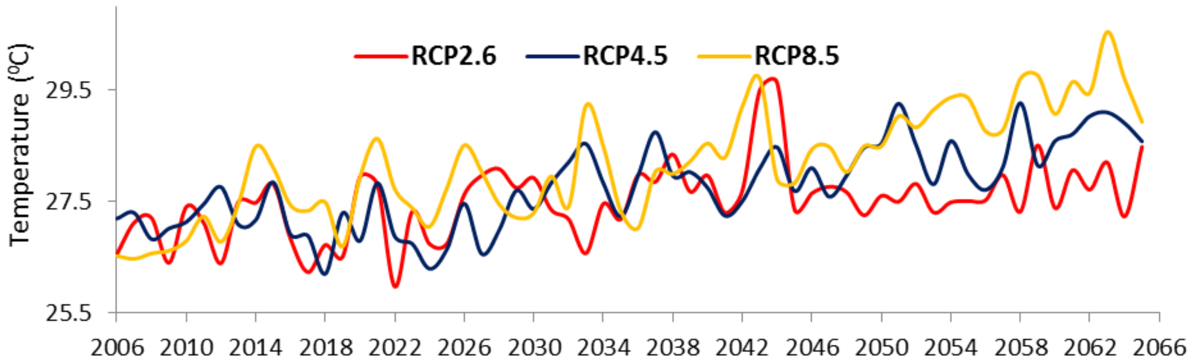

Fig3.5: Trend in Tmax projected during 2006-2065 under RCP2.6, RCP4.5 and RCP8.5

In a short period projection, almost all the future projection of maximum temperature under RCP 2.6 has shown increasing trend for all months However, in short term forecast, there is a probability of February and May temperature to be decreased by 0.54% and 3.04% respectively. In a mid-term forecast, relatively the highest absolute mean monthly difference from the baseline temperature is found at the month of November. This indicates a temperature increase by 1.36 oC (6.68%) at the end of 2050. In general, the annual maximum temperature may increase by 0.38 oC, 0.96 oC and 0.77 oC at the end of 2035, 2050 and 2065 respectively. Fig 3.6 presents the mean monthly maximum temperature fluxes under RCP 2.6 scenario as compared to the base period.

In a mid-term and long-term forecast all the climate projections has revealed absolute change in maximum temperature under RCP4.5. The highest temperature increment will be expected on July, which might be attained at the end of 2065. The change may exceed 2.33 ^oC.

In general, the intermediate scenario, which considers an averaged population growth and development, the mean annual maximum temperature may increase by 0.15^0C, 0.84^0C and 1.350C at the end of 2035, 2050 and 2065 respectively. Fig 3.7 shows the percentage change in mean monthly maximum temperature under RCP 4.5 scenario as compared to the base period.

The scenario with very high GHG emission, RCP8.5 revealed absolute change in maximum temperature for all projections. The highest temperature increment will be expected on June, which will be expected to increase by 3.04 ^oC at the end of 2065. In general, under RCP8.5 scenario, the mean annual maximum temperature may increase by 0.57 ^0C, 1.12 ^0C and 2.12^0C at the end of 2035, 2050 and 2065 respectively. Fig 3.8 shows the percentage change in mean monthly maximum temperature under RCP 8.5 scenario as compared to the base period.

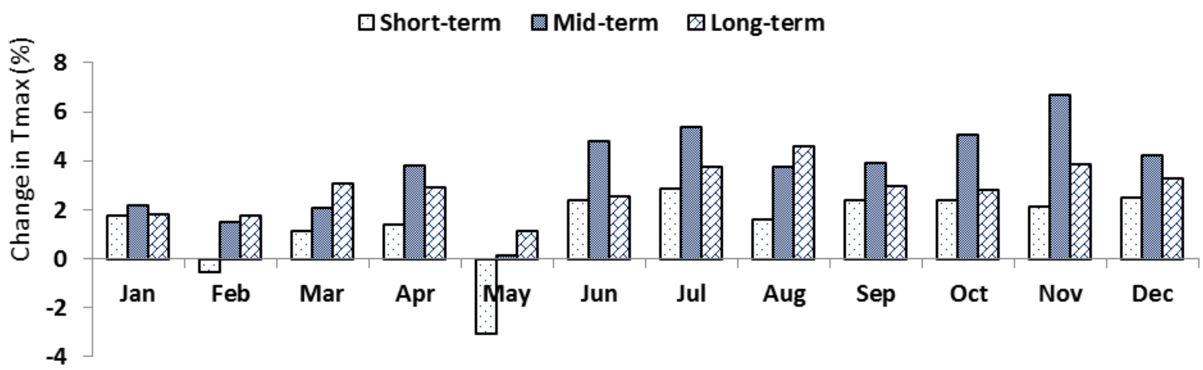

Fig3.6: Mean monthly maximum temperature fluxes under RCP 2.6 scenario as compared to the base period.

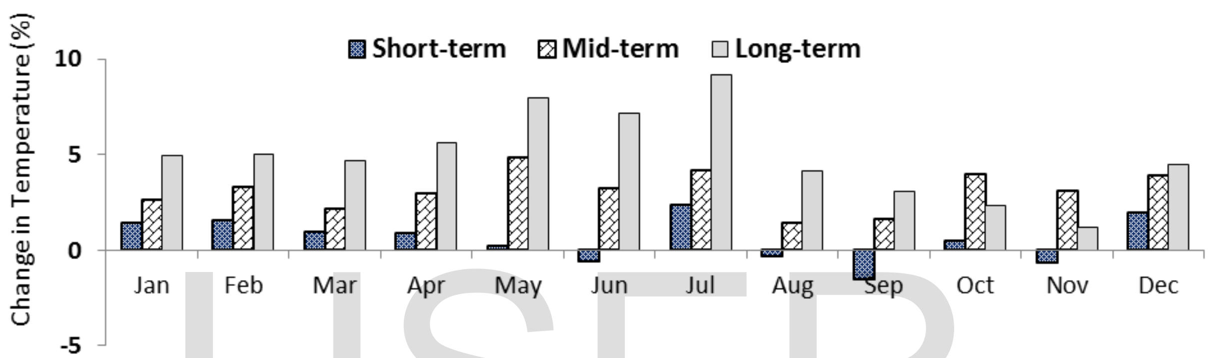

Fig3.7: Mean monthly maximum temperature fluxes under RCP 4.5 scenario as compared to the base period.

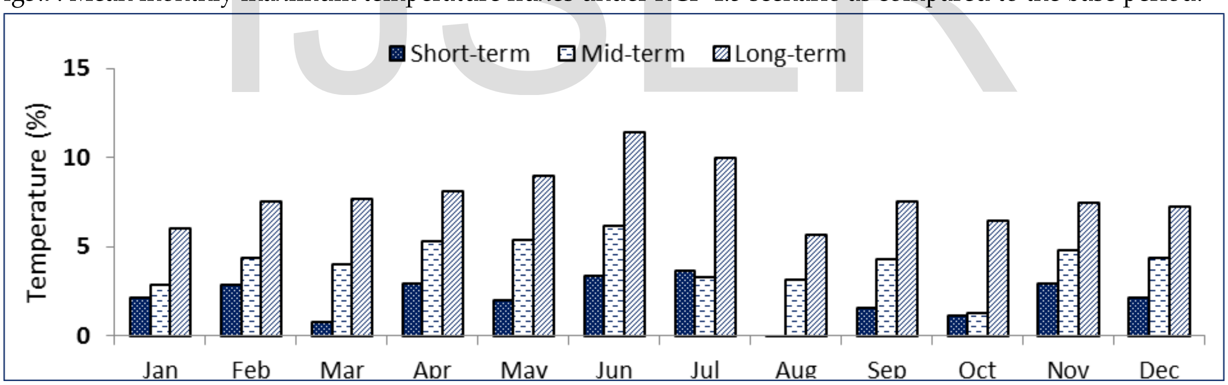

Fig3.8: Mean monthly maximum temperature fluxes under RCP 8.5 scenario as compared to the base period.

Minimum Temperature Scenario: Minimum temperature projection shows an absolute increasing trend for all the three scenarios. When compared to the maximum temperature and precipitation flux, the increase in minimum temperature is very high for all the climate projections.

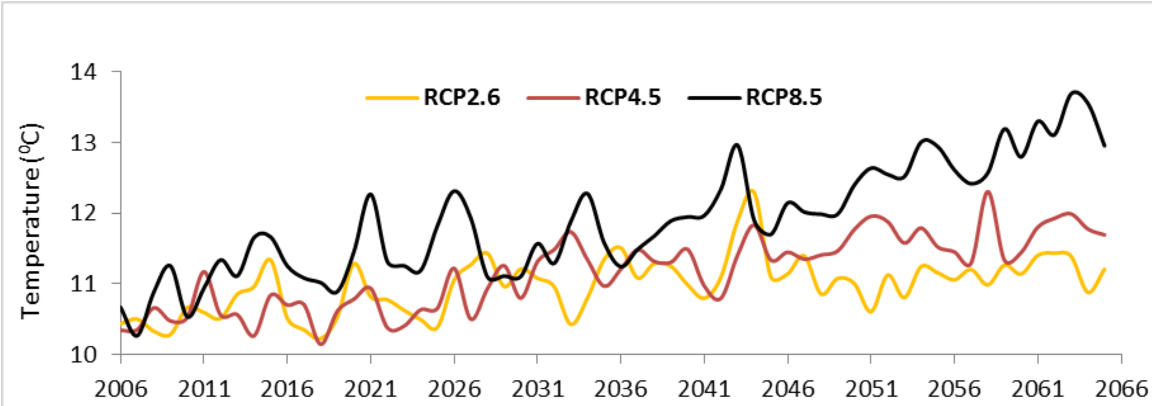

Fig3.9: Trend in Tmin observed during 2006-2065 under RCP2.6, RCP4.5 and RCP8.5

In mid-term and long-term projections, all the future projection of minimum temperature under RCP 2.6 has shown increasing trend for all months. In a long term forecast during April and December alone the minimum temperature is expected to increase by 0.700C and 0.53 0C at the end of 2065 respectively. In general minimum temperature projection under the stringent GHG emission has revealed increase by 0.360C, 1.390C and 2.310C for short-term, mid-term and long-term projections respectively.

The entire future projection of minimum temperature under RCP 4.5 indicates increasing trend for all months. During April and December the minimum temperature is expected to increase by 0.700C and 0.53 0C respectively. In general minimum temperature projection under the medium GHG emission has revealed increase by 0.340C, 0.74 0C and 1.100C for short-term, mid-term and long-term projections respectively.

The future projection of minimum temperature under RCP 8.5 indicates increasing trend for all months. Under this scenario, at the end of 2065 minimum temperature increment tends to reach 1.460C and 1.8 0C in February and November respectively. In general minimum temperature projection under the highest GHG emission scenario has revealed increase by 0.250C, 1.81 0C and 1.810C at the end of 2035, 2050 and 2065 respectively

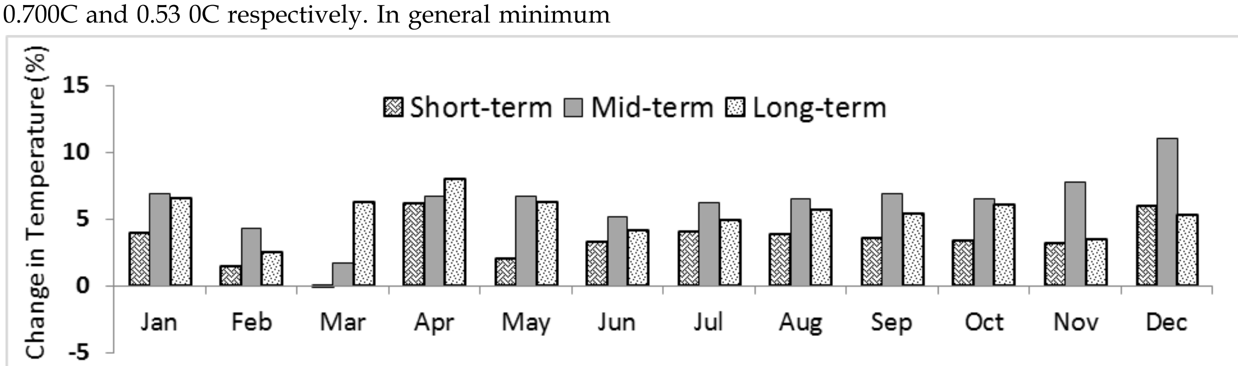

Fig3.10: Mean monthly minimum temperature fluxes under RCP 2.6 scenario as compared to the base period.

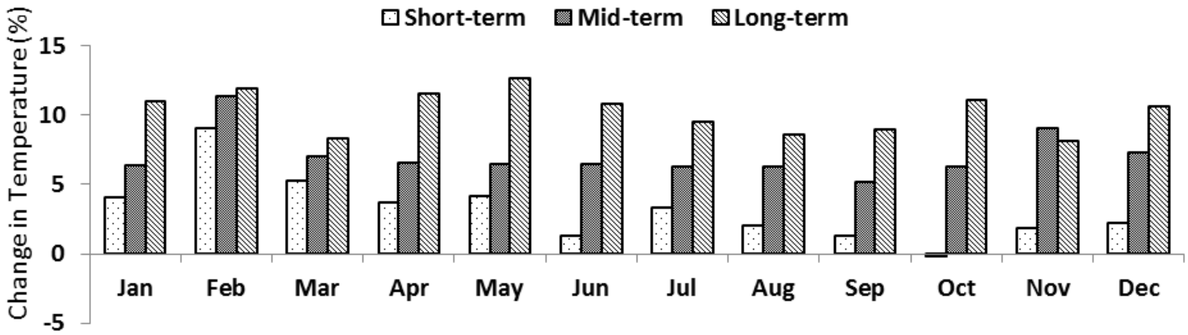

Fig3.11: Mean monthly Tmax fluxes under RCP 4.5 scenario as compared to the base period

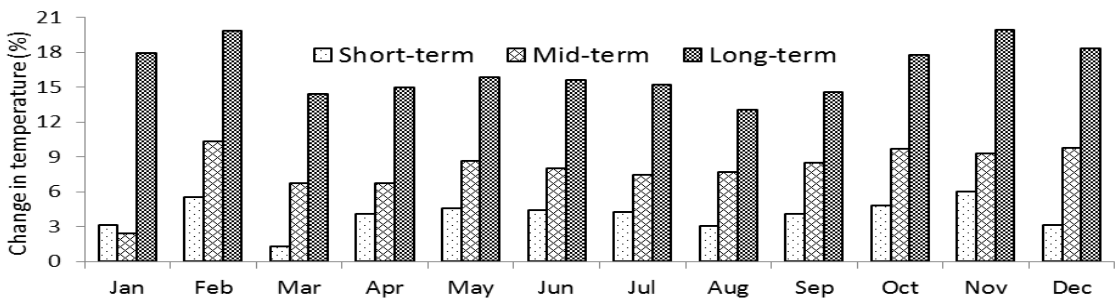

.

Fig3.12: Absolute mean monthly Tmin fluxes under RCP 8.5 scenario as compared to the base period

3.3 HBV-Hydrological model result

The rainfall-runoff modeling was conducted using HBV model. Firstly the performance of the model was evaluated by using hydrograph comparison at Abelti gauge station through calibration and validation. Secondly using the optimized parameters at Abelti station, the flow for the ungauged catchment was estimated. Finally, by using Muskingum channel routing method, flow from Abelti, Gojeb and Wabe basins were routed and summed up with ungagged basin flow at Gibe-III dam site. For Gibe–III basin, since the ungagged part was very large in comparison to the gauged basin, the parameters obtained at Abelti gauge station were re-evaluated (validated) by generating flow at Gibe-III against the sum of flow from all the basins. Calibration aimed at the water balance and over all shape agreement of the observed discharge was evaluated using NSE, D and R2.Flow calibration at Abelti gauge station was done by using hydro-meteorological data of 1985-1994 whereas validation was done by using 1995-2002 data.

Flow calibration at Abelti gauge station

Flow calibration was done by using the observed daily areal rainfall, long years mean monthly temperature, long years mean monthly Evapo-transpiration, mean daily temperature and observed flow at Abelti gauging station. On a daily basis, Calibration at Abelti gauging station resulted with a NSE of 0.77, R2 of 0.77 and D of 0.21%. On monthly basis, NSE of 0.84, R2 of 0.84 and percentage volume difference, D of 0.23% was obtained. These values demonstrate that the model has a very good capability to simulate the observed flow for both low flow and high flow periods.

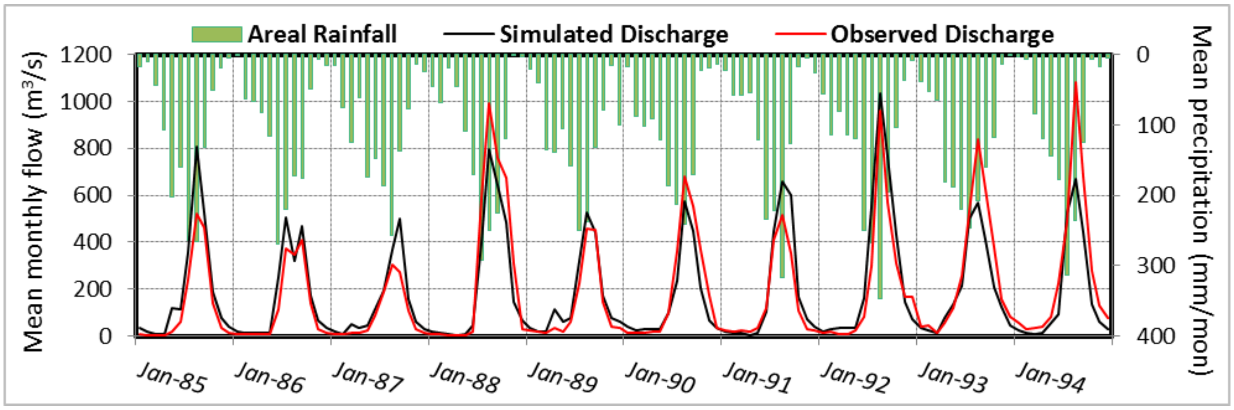

Fig3.13: Mean monthly hydrograph comparison calibration result at Abelti gauge station

Flow validation at Abelti gauging Station

Validation of the model parameter was verified by using different time from calibration periods. The same efficiency evaluation techniques during calibration were implemented. On daily basis, flow validation at Abelti gauging station resulted with a NSE of 0.75, R^2 of 0.75, and D of -0.93%. On a Monthly basis observed flow comparison against simulated discharge resulted with a NSE of 0.81, R2 of 0.82, and D of -2.80%.These values indicate that the model parameters obtained were stable; hence the model can be used for future inflow generation.

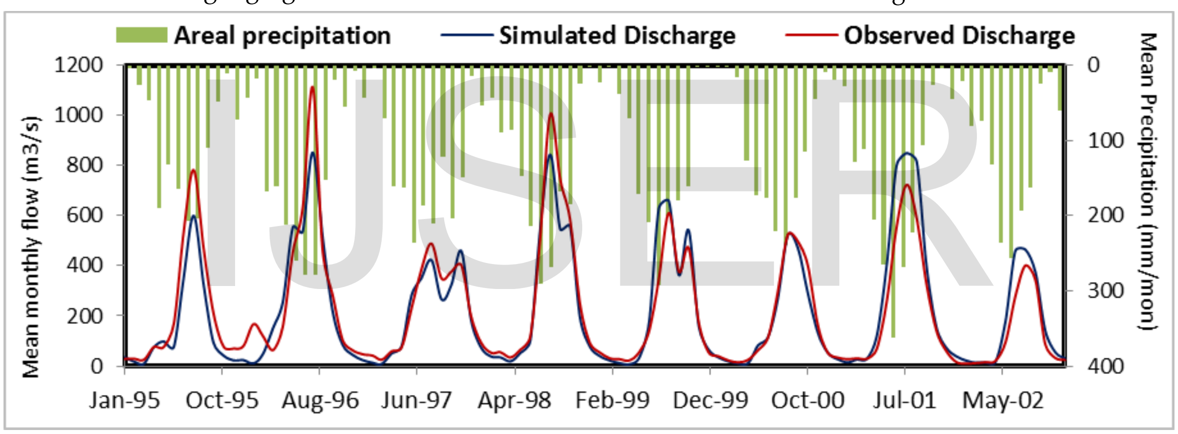

Fig 3.14: Mean monthly hydrograph comparison during validation at Abeltiguaging station

The calibration and validation results show good shape agreement between the observed and simulated flow at Abelti gauge station(Fig. 3.15). Hence, the model has very good capacity in reproducing the observed flow with certain limited uncertainties.

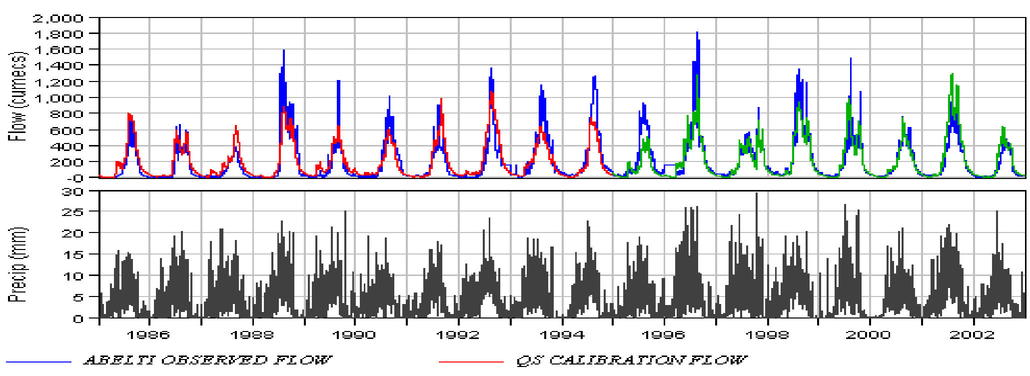

Fig3.15: Daily hydrograph comparison of observed flow against simulated flow (1985-2002)

ISSN 2229-5518

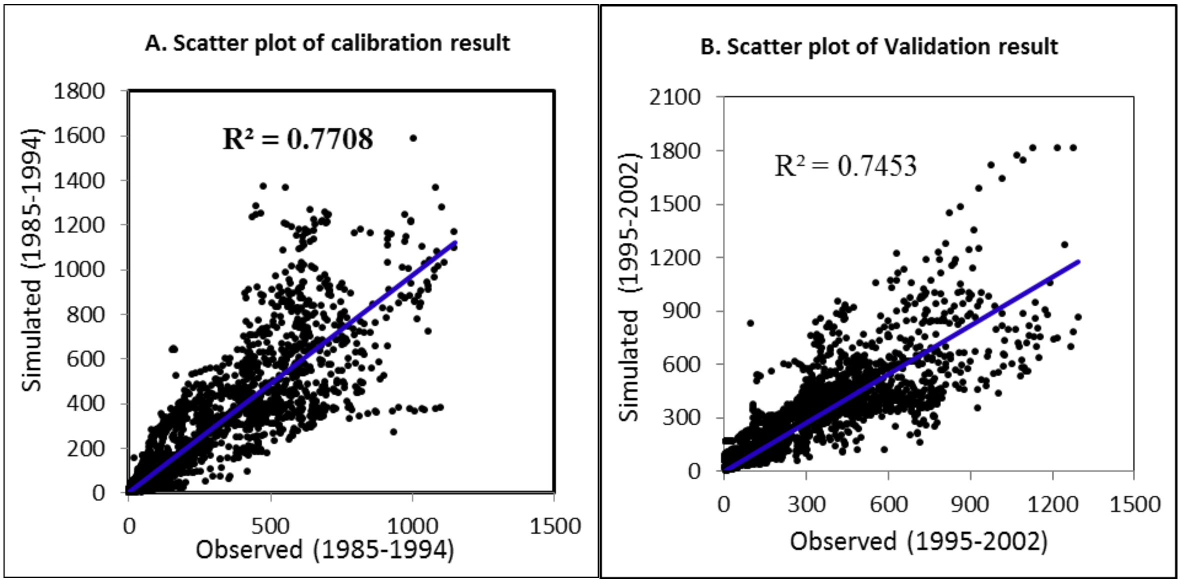

Fig 3.16: Scatter plot of observed against simulated flow during calibration (A) and during validation (B)

Flow validation at Gibe-III near dam site

The ungagged catchment in Gibe-III river basin is much larger than the gauged part. In such catchments transposing flow from the gauged catchment by using area ratio method is impossible. Hence, implementing different techniques evaluating and confirming the suitability of parameters obtained at Abelti for Gibe-III basin is important. To achieve this goal we implemented a Muskingum Channel Routing technique:

Muskingum Channel Routing: In this method, flows from the upper catchments were routed to obtain an approximate observed flow at Gibe-III near dam site. Firstly, the observed flow from Abelti, Wabe and Gojeb were routed in to Gibe-III near dam site. Then the routed flow from each basin were summed up with the ungagged basin flow at Gibe-III near dam site and compared with the generated discharge using HBV-model at Gibe-III dam site. Finally, the hydrograph from the two methods was checked for model validity.

In general, meteorological data from 1985-2004 (20 years) were used to generate flow near Gibe-III dam site. Using an equal length of flow data, flow from each basin was routed and summed up at Gibe-III dam site including the ungagged basin flow. The result between the routed and generated flow has revealed NSE of 0.91, R2 of 0.91, and D of -1.41% on a daily basis. On a monthly basis routed flow comparison against simulated discharge has resulted with a NSE of 0.94, R2 of 0.94, and D of –1.40%. The model simulation was done by using the optimized parameters for Abelti basin by only changing the watershed area and editing the length of simulation period from ten year to fifteen years.

Fig 3.17 presents the result of hydrograph comparison for the year 1985-2004.As it is observed the graph shows as the overall shape agreement was obtained between the generated and routed flow in to Gibe-III reservoir.

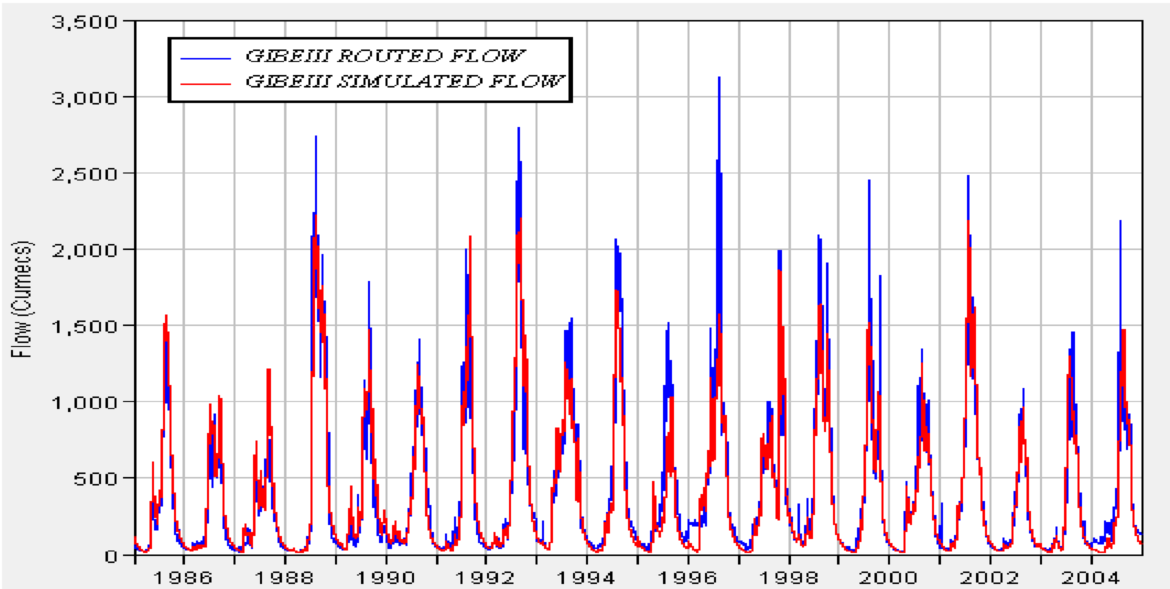

Fig3.17: Hydrograph Comparison for generated and routed flow at Gibe-III near dam site

The scatter plot of generated and simulated flow for verification (1985-2004)was presented in Fig 3.21. The trend line reveals better correlation coefficient than calibration and validation.

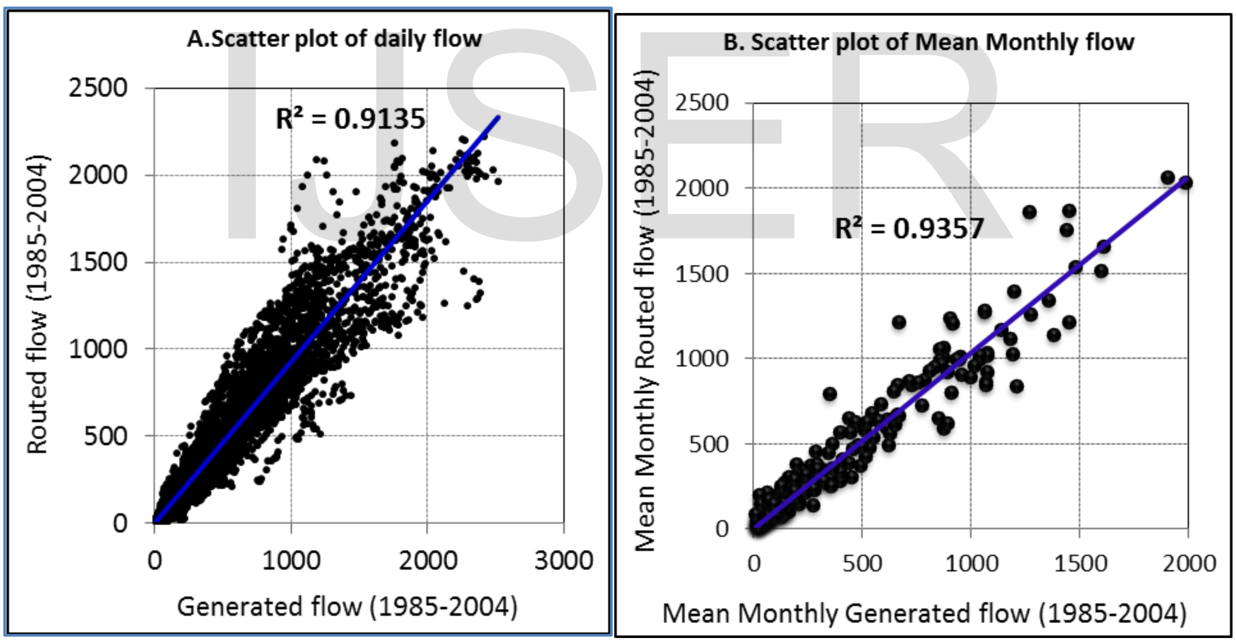

Fig 3.18: Scatter plot of mean monthly and daily generated against routed flow during at Gibe-III near dam site

3.4 Net Reservoir Inflow Volume

Reservoir Inflow volume mainly depends up on the catchment characteristics like rainfall, evapo-transpiration, temperature and etc. Therefore, if change in any one of these characteristics is observed, there is a big probability that the reservoir volume may change. For this study, keeping the other entire factors constant in the future, Gibe-III reservoir inflow volume variation was estimated by using the future climate variables change. Like precipitation change, climate projection of reservoir inflow didn't manifest systematic change. Reservoir inflow volume change has shown high flux throughout the entire season.

The future reservoir inflow was generated by using HBV hydrological model. For comparison purpose, the reservoir inflow volume was generated for the base period (2006-2020) and three future periods called short-term (2021-2035), mid-term (2036-2050) and long term (2051-2065).

To obtain the net inflow volume in to Gibe-III reservoir, firstly the evaporation loss from Gibe-I and Gibe-III reservoir was estimated from the nearby stations to each reservoir. Accordingly, the nearest meteorological station to Gibe-I reservoir was Jimma station where as Hossana and Wolaita stations are the closest stations to Gibe-III reservoir. The average maximum and minimum temperature data from Hossana and Wolaita station were used to estimate the evaporation loss from Gibe-III reservoir. To obtain the mean monthly evaporation loss (Mm3/m) from each reservoir, the monthly evaporation loss (mm/mon) from each reservoir was multiplied by their corresponding full supply level (FSL) reservoir surface area. Thereafter, the sum of the two evaporation value was deducted from the generated mean monthly flow at Gibe-III near dam site using HBV-model.

Table3.1: shows the calculated reservoir loss due to evaporation corresponding to future time horizon

	Evaporation loss from Gibe-III (Mm3/month)			Evaporation loss from Gibe-I (Mm3/month)			Total Evaporation Loss (Mm3/m)		
	RCP2.6	RCP4.5	RCP8.5	RCP2.6	RCP4.5	RCP8.5	RCP2.6	RCP4.5	RCP8.5
Jan	32.11	31.17	31.24	9.13	9.10	9.19	41.24	40.27	40.43
Feb	31.70	30.54	30.33	8.92	8.99	8.99	40.61	39.53	39.32
Mar	36.09	35.58	35.30	9.94	10.52	10.53	46.03	46.10	45.83
Apr	33.39	32.66	32.91	8.71	9.51	9.69	42.10	42.16	42.60
May	33.11	32.51	32.55	8.11	9.38	9.49	41.21	41.89	42.04
Jun	28.90	30.45	29.69	6.67	8.38	8.20	35.57	38.83	37.89
Jul	27.26	28.65	28.88	6.86	7.62	7.78	34.11	36.28	36.65
Aug	27.62	28.98	28.97	7.00	7.79	7.88	34.62	36.78	36.85
Sep	28.34	29.72	29.14	7.04	8.17	8.06	35.39	37.89	37.20
Oct	30.37	31.18	31.10	7.84	8.64	8.77	38.21	39.82	39.87
Nov	28.99	29.74	29.02	8.12	8.60	8.46	37.11	38.34	37.49
Dec	30.50	29.87	29.93	8.78	8.76	8.82	39.29	38.63	38.76
Mean	30.70	30.92	30.75	8.09	8.79	8.82	38.79	39.71	39.58
Sum	368.39	371.05	369.06	97.12	105.47	105.86	465.51	476.52	474.92

At the end of 2065, the mean annual evaporation loss from Gibe III reservoir having surface area of 211.64km2 at its FSL is projected to be 368.39Mm3, 371.05Mm3 and 369.06Mm3 for RCP2.6, RCP4.5 and RCP8.5 scenarios respectively. This indicates a loss of 11.68 m3/s, 11.77 m3/s and 11.73m3/s for RCP2.6, RCP4.5 and RCP8.5 scenarios respectively. For Gibe-I, the mean annual evaporation loss at its FSL (60.1Km2) is projected to be 97.12Mm3, 105.47Mm3 and 105.86Mm3 for RCP2.6, RCP4.5 and RCP8.5 scenarios respectively. The corresponding loss is about 3.08 m3/s, 3.344 m3/s and 3.57m3/s for RCP2.6, RCP4.5 and RCP8.5 scenarios respectively. This value will be deducted from the inflow generated by using HBV-model. Table 3.2 shows the net inflow volume calculated by subtracting the total evaporation loss from each reservoir.

Table 3.2: Net mean annual inflow to Gibe-III reservoir

	Inflow Generated (Mm3/m)			Reservoir Evaporation Loss(Mm3/m)			Net- inflow volume (Mm3/m)		
	RCP26	RCP45	RCP85	RCP26	RCP45	RCP85	RCP26	RCP45	RCP85
Jan	134.0	177.4	139.2	41.2	40.3	40.4	92.8	137.2	98.8
Feb	230.0	227.5	119.0	40.6	39.5	39.3	189.4	187.2	79.7
Mar	164.5	131.9	122.7	46.0	46.1	45.8	118.5	85.8	76.9

Apr	152.1	206.0	117.3	42.1	42.2	42.6	110.0	163.8	74.7
May	536.7	438.8	301.3	41.2	41.9	42.0	495.5	396.9	259.3
Jun	1887.5	1539.12	1346.2	35.6	38.8	37.9	1851.9	1500.2	1308.3
Jul	2149.2	1998.6	1610.9	34.1	36.3	36.7	2115.1	1962.3	1574.3
Aug	2981.0	3225.6	2962.3	34.6	36.8	36.8	2946.4	3188.8	2925.4
Sep	2025.6	2268.7	1889.8	35.4	37.9	37.2	1990.2	2230.8	1852.6
Oct	1361.9	1390.2	1283.0	38.2	39.8	39.9	1323.7	1350.4	1243.2
Nov	481.3	634.6	516.9	37.1	38.3	37.5	444.1	596.3	479.4
Dec	228.3	272.3	241.8	39.3	38.6	38.8	189.0	233.7	203.1
Mean	1027.7	1105.5	887.5	38.8	39.7	39.6	988.9	1065.8	848.0
Sum	12332.2	13266.0	10650.5	465.5	476.5	474.9	11866.7	12789.4	10175.6

The projected net inflow volume to Gibe III reservoir corresponding to 2020 to 2065 from RCP2.6 scenario shows decreasing volume by 14.02% which shows fall in inflow volume from 13802 Mm3/year in 2006-2020 to 11866.7Mm3/year at the end of 2065., Like precipitation scenario, mean monthly variation is highly pronounced. For instance RCp2.6 scenario projected a decreased volume by 44.3%, 52.06% and 44.57% during November, January and March respectively as compared with base period. In general, for RCP2.6, low flow seasons, NDJ and FMA have shown high fluxes whereas high flow season JAS didn't show big difference as compared to the base period.

RCP4.5 scenario with an average GHG emission scenario has revealed decreasing volume by 2.28% which shows decrease in annual inflow volume 282.2 Mm3/m at the end of 2065. Like RCP2.6 mean monthly variation is highly pronounced. For instance, the projection of net inflow volume a decreased volume by 47.02% is expected whereas an increase in net inflow volume by 78.6% is expected during March and February respectively as compared with base period. In general, low flow seasons, has shown high fluxes than low flow seasons.

RCP8.5 net inflow Scenario: RCP8.5 scenario, the highest GHG emission scenario has revealed decreasing volume by 13.3% which shows decrease in annual inflow volume 1556.2 Mm3/m at the end of 2065. Except in August and October, the future projection of net inflow volume for RCP8.5 scenario has revealed decrease in volume. The maximum decrement 64.02% is in February and the increment of 5.05% may occur in October. Fig 3.19 shows Change in mean monthly net inflow volume to Gibe-III reservoir as compared to base period 2006-2020.

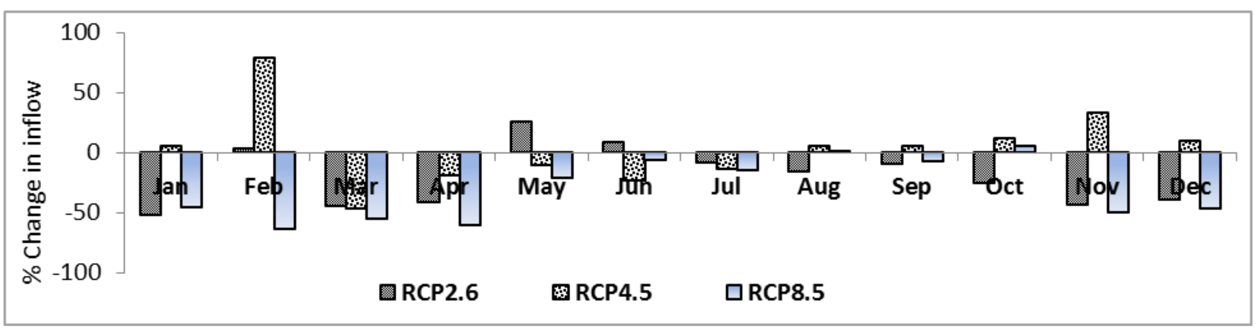

Fig3.19: Change in mean monthly net inflow volume at 2065 as compared to base period

3.5 Evaluating the performance indices of Gibe-III reservoir

After generating the reservoir inflow, the performance of Gibe-III reservoir is examined by using four performance indices under the standard operation policy of the reservoir. Both current and future generation inflow are considered during quantifying the performance indices. For the sake of comparative purpose the indices also examined without the reservoir existing condition.

Time based and volumetric reliability

The averaged time-based reliability of the Gibe-III reservoir reveals a value of above 50% for both RCP2.6 and RCP4.5 scenarios under all the three time horizons. But less value was observed for RCP8.5 specifically in short-term and mid-term forecast. A value of 100% time based reliability can be explained as, the reservoir can meet the target demand for all its simulation period. Actually, slight increase in the time based reliability is observed, when the reservoir simulation is done by starting the reservoir with its full supply level than starting from the reservoir empty condition. On average this time based reliability decreases to 24.2 % for no reservoir conditions from 69.3% of reservoir existing condition.

The volumetric reliability describes the total volume water supplied to the reservoir or demand site i.e. the value of volumetric reliability index indicts that, how much the supplied volume of water can meet the required volume of demand. A 100 % of volumetric reliability index of reservoir tells that there is no shortage for the reservoir to meet the demanded from the volume (amount) point of view. The result of the analysis for the study area reveals that the annual average volumetric reliability is above 43% for no reservoir conditions and above 80 % for reservoir existing condition. The result value of above 80% tells there exists very good potential at the site to meet the demand in terms of volume. For the case of Gibe-III reservoir the value 43% without reservoir condition indicates that the reservoir cannot supply the total volume required by targeted demand. With reservoir existing condition beginning from full supply level, an average volumetric reliability of 81.5% was obtained for the stringent and averaged GHG emission scenario; whereas most probably, the potential of the reservoir under the highest GHG emission scenario indicates less capacity of the reservoir to meet the target demand.

Resilience of Gibe-III Reservoir (φ)

The Gibe-III reservoir resilience which is the indication of how quickly the reservoir system recovers its self from failing to meet the targeted demand to fully satisfy the required demand exhibits a percentage value of less than 35%, for all the climate scenarios. This value indicates that the reservoir has very slow speed of recovery, to meet the demand once the failure to meet the target demand is occurred. A value of 100% resilience indicates the reservoir system will recover itself from failure to meet the target demand with in very short period of time.

Dimensionless Vulnerability (η)

The average dimensionless vulnerability of the Gibe-III reservoir goes up to 22.7 % for no reservoir condition and it will reach up to 43.2 % with reservoir condition. A 100 % of dimensionless vulnerability reflects that the reservoir face a shortage of flow to meet the demand in all simulation period.

Table3.3: Performance indices for no reservoir and with reservoir existing conditions

Scenarios	Period	Without storage				With Storage starting from empty condition			
		Rt	Rv	Re	η	Rt	Rv	Re	η
RCP2.6	Base period	30.8	53.1	14.5	12.1	82.5	87.6	23.8	23.8
	2021-2035	30.0	51.0	16.7	11.9	60.8	74.1	23.4	17.0
	2036-2050	26.7	46.0	13.6	12.5	62.5	73.6	15.6	22.2
	2051-2065	24.2	45.3	14.3	11.0	55.8	69.3	17.0	17.0
RCP4.5	Base period	26.7	49.8	12.5	22.7	63.3	78.0	15.9	43.2
	2021-2035	32.5	51.4	13.6	12.4	77.5	84.0	22.2	25.9
	2036-2050	25.8	48.0	12.4	12.4	75.0	83.5	16.7	30.0
	2051-2065	26.7	50.9	17.0	12.5	64.2	79.5	25.6	16.3
RCP8.5	Base period	27.5	45.9	14.9	10.3	57.5	69.4	17.6	13.7
	2021-2035	20.8	43.9	11.6	11.6	40.0	59.6	13.9	13.9
	2036-2050	21.7	43.2	16.0	10.6	45.8	61.6	13.8	13.8
	2051-2065	22.5	44.6	11.8	10.8	60.0	73.9	18.8	20.8

Table3.4: Performance indices for the reservoir under different scenarios with the analysis start at reservoir empty level

Scenarios	Period	With storage and Reservoir full condition				
		Rt	Rv	Re	η	Elevation(m)
RCP2.6	Base period	91.7	94.1	30.0	50.0	892.0
	2021-2035	74.2	81.9	22.6	25.8	892.0
	2036-2050	76.7	83.6	17.9	35.7	892.0
	2051-2065	70.0	79.3	16.7	25.0	892.0
RCP4.5	Base period	68.3	81.7	15.8	47.4	892.0
	2021-2035	90.0	93.3	25.0	41.7	892.0
	2036-2050	88.3	92.6	14.3	64.3	892.0
	2051-2065	77.5	89.5	33.3	22.2	892.0
RCP8.5	Base period	70.8	79.4	20.0	17.1	892.0
	2021-2035	53.3	69.5	14.3	17.9	892.0
	2036-2050	57.5	71.6	13.7	17.6	892.0
	2051-2065	71.7	81.9	17.6	29.4	892.0

4. CONCLUSSION AND RECOMMENDATION

4.1 Conclusions

In this study the Gibe-III reservoir performance under the climate change was quantified by using the reliability, resilience and vulnerability indices (RRV-criteria). The reservoir inflow to Gibe-III dam site was estimated by transferring the runoff from Great Gibe at Abelti, Gojeb near Shebe and Wabi at Wolkite gauged stations and Ungauged basin by using Muskingum flood routing techniques. The overall water resources availability for current and future time period under climate change scenarios were generated by using calibrated and validated HBV-model. Based on the study the following conclusions are drawn;

The result of climate projection using statistically downscaled and bias corrected CORDEX data using power transformation technique has shown very good ability to replicate the historical maximum and minimum temperature for the observed period; but less for the observed precipitation with the simulated precipitation.

Generally the projected maximum and minimum temperature shows an increasing trend at the end of 2065. Except for RCP4.5, the precipitation projection shows decreasing trend for RCP2.6 and RCP8.5 when compared to the base period. All the projected maximum and minimum temperature are within the limits of the expected projection carried by the latest IPCC, 2014.

The HBV model which is calibrated and validated in a daily time step was used to simulate the observed discharge. To obtain the optimal model parameters, calibration and validation was done at Abelti basin. Then, using these parameters, the performance of the model was re-evaluated at Gibe-III near dam site. In general, the model has simulated the observed discharge reasonably in a well manner with the model performance criteria of Nash and Sutcliffe value NSE=0.77 during calibration and R2= 0.75 during validation.

For all the climate scenarios, future projection of climate shows decreasing trend. At the end of 2065, the generated net inflow volume to the reservoir shows an average annual decrease in volume by 14.02%, 2.28% and 13.3% under RCP2.6, RCP4.5 and RCP8.5 respectively. In comparison to the other scenarios, RCP4.5 decrement is less because precipitation projection has shown small increment for some of the periods.

The performance of the reservoir was evaluated by reliability, resilience and vulnerability (RRV) indicators. The reliability index of Gibe-III reservoir for all climate scenarios reveals above 75%, hence it is concluded that the reservoir has a reasonably good capacity to meet the required target demand at the end of 2065.

In general from performance indices of the reservoir, the decision makers, concerned persons or any reservoir water users can be assured that the reservoir has very good potential to generate the required power under future climatic condition with the consideration of described research limitations.

4.2 Recommendation

Generally from this specific study the following three main points are recommended;

In order to assure the development of water resource and energy production capacity of developing countries like Ethiopia, further studies which incorporate the impact of climate change with land use and land cover change, plus sediment inflow to the reservoirs should be undertaken by using more than one and more finer resolution of Global Circulation Models (GCMs). These studies should also investigate the adaptation options for the impact of climate change consequences.

This study has not considered land use/land cover change and seepage from the reservoir; therefore, quantification and simulation of seepage from the reservoir can alter result obtained from HBV and RRV performance of the reservoir. Therefore, the study recommend including this parameter in future studies.

To make the evaluation of climate change impact more complete, it is appreciable to use other physically based regional downscaling methods with the addition of other performance indices, such as Drought Risk Index (DRI) and Sustainability Index.

Acknowledgment

Mr. Ayana thanks the Ministry of Water Irrigation and Electricity (MoWIE) for the financial support during the period of undertaking this research. He is further grateful to Arba Minch University, Institute of Technology (Ethiopia).

References

[1] Abdella Kemal (2014). The Effect of Climate Change on Water Resources Potential of Omo Gibe Basin, Ethiopia. PhD. Dissertation, Munich, Germany.

[2] Allen (1995). Evaluation of procedures for estimating grass reference evapotranspiration using air temperature data only. Water Resources Development and Management Service. Land and Water Development Division. United Nations Food and Agriculture, Rome, Italy.

[3] Avery,S (2012. Lake Turkana and the Lower Omo: Hydrological Impacts of A Major Dam and Irrigation Development, Vol, I African Studies Center, Oxford University.

[4] Awulachew, S. B., Yilma, A. D., Leulseged, M., Loiskandl, W., Ayana, M., Alamirew, T. (2007). Water resources and irrigation development in Ethiopia. Colombo, Sri Lanka: international water management institute. 78p. (Working Paper 123) ISBN 978-92-9090-680-3

[5] Awulachew, S. B et al, Water Resources and Irrigation Development in Ethiopia, Colombo, Sri Lanka: International Water Management Institute. 78p. (Working Paper 123) 2007.

[6] Babazadeh, Performance evaluation of Jiroft storage dam Operation using HEC-RESSIM 2.0, Tehran-Iran: Eleventh International Water Technology Conference, IWTC11 2007 Sharm El-Sheikh, Egypt PP449

[7]

[8] Bates B., Kundzewicz C., Wu W., Palutikof P. (eds) (2008). Climate change and water. Technical Paper of the Intergovernmental Panel on Climate Change. Geneva, Switzerland, IPCC Secretariat, P 210.

[9] Brekke, D. Levi, et al (2009), Climate Change and Water Resources Management: A Federal Perspective, USGS Circular 1331.

[10] Brooks PD, Troch PA, Durcik M, Gallo E, Schlegel M etal. Quantifying regional scalevegetation response to changes in precipitation: Not all rain is created equal. Water Resources Research 47: W00J08, DOI: 10.1029/2010WR009762. 2001.

[11] Boko M., I. Niang, A. Nyong, C. Vogel, C. A. Cutheko, M. Medany, B. Osman-Elasha, R. Tobo, P. Yonda, "Af-rica in: Parry in Canzianio," In: J. Palutikof, P. Vander Lenden and C. Harison, Eds., Climate Change (2007). Impacts, Adaptation and Vulnerability. Working Group II Contribution to the Fourth Assessment Report of the Intergovernmental Panel on Climate Change, Cambridge University Press, Cambridge, pp. 433-467.

[12] DeepashreeRaje and Mujumdar, (2009). Reservoir performance under uncertainty in hydrologic impacts of climate change. Advances in Water Resources 33 (2010) PP312–326

[13] EEPCo (2004). Ethiopian Electric Power Corporation, Gilgel Gibe Hydroelectric power plant Information booklet, An EEPCo Publication, Addis Ababa, Ethiopia, 28 pp.

[14] EEPCo (2007). Ethiopian Electric Power Corporation, Gibe III Hydroelectric Project, Reservoir seepage risk analysis, An EEPCo Publication, Addis Ababa, Ethiopia, 82 pp.

[15] EEPCo (2009) Gibe III Hydroelectric Project, Environmental & Social Impact Assessment, CESI & Mid-Day International, 300 ENVRC002C, An EEPCo Publication, Addis Ababa, Ethiopia, 351 pp.

[16] Fasil (2013). Hydrologic partitioning and vegetation response in selected moist zone catchments of Ethiopia: analyzing spatiotemporal variability." M.Sc. Thesis, Ethiopian Institute of Water Resources, Addis Ababa, Ethiopia.

[17] Hall, and Dahmen ER (1990). Screening of HydrologicalData: Tests for Stationarity and Relative Consistency. International Institute for Land Reclamation and Improvement/ILRI. Publication 49.

[18] Hunt A, Watkiss P (2011). Climate change impacts and adaptation in cities: a review of the literature. 104:13–49. doi:10.1007/s10584-010-9975-6

[19] IPCC, (2010), statement on the melting of Himalayan glaciers. A statement from the Chair and Vice-Chairs of the IPCC, and the Co-Chairs of the IPCC Working Groups

[20] IPCC, (2001). Climate Change 2001: The Scientific Basis. Contribution of Working Groups I to the Third Assessment Report of the Intergovernmental Panel on Climate Change [Houghton, J.T.,Y. Ding, D.J. Griggs, M. Noguer, P.J. van der Linden, X. Dai, K. Maskell, and C.A. Johnson (eds.)]. Cambridge University Press, Cambridge, United Kingdom and New York, NY, USA, 881pp.

[21] IPCC, (2007). Climate Change 2007: Impacts, Adaptation and

Vulnerability. Contribution of Working Group II to the Fourth Assessment Report of the Intergovernmental Panel on Climate Change, M.L. Parry, O.F. Canziani, J.P. Palutikof, P.J. van der Linden and C.E. Hanson, Eds., Cambridge University Press, Cambridge, UK, 976pp.

[22] IPCC, (2010), statement on the melting of Himalayan glaciers. A statement from the Chair and Vice-Chairs of the IPCC, and the Co-Chairs of the IPCC Working Groups

[23] IPCC, (2014). Climate Change 2014: Impacts, Adaptation and Vulnerability. Contribution of Working Group I-IV to the Fifth Assessment Report of the Intergovernmental Panel on Climate Change, Rajendra K. Pachauri, Leo Meyer and Vicente R. Barros, IPCC, Geneva Switzerland, 151pp.

[24] Neupane, K. Establishing Community Based Early Warning System Practitioner's Handbook, Mercy Corps and Practical Action, SanepaChowk, Lalitpur, Nepal,2010

[25] Richard Woodroofe& associates, (1996), Omo-Gibe River basin Integrated Development Master Plan Study Final Report Vol. VI Water resources Surveys and Inventories, ministry of Water Resources, A.A.

[26] Senay (2012). Assessing the potential hydrological impact of the Gibe III Dam on Lake Turkana water level using multi-source satellite data. Hydrology and Earth system Science .doi:10.5194/hess-16-3561-2012. Pp3561-3578.

[27] Seyum,T.et al. SWAT Hydrologic Modeling and Simulation of Inflow to Cascade Reservoirs of the semi-ungaugedOmo-Gibe River Basin, Ethiopia, Department of Geo-hydraulics and Engineering Hydrology, Kassel University,2013 Kassel.

[28] Shiferaw, T. Elias, Climate change induced Spatio-temporal hydrological variability on Omo-Gibe River Basin of Ethiopia, Ethiopian Institute of Water resources, Addis Ababa, Ethiopia.

[29] SNNPR, Rescue, resource mobilization and rehabilitation Committee, South Omo Floods, Flass Appeal Report, 2006 Hawassa.